

B. Stieler and H. Winter
Deutsche Forschungs- und Versuchsanstalt für Luft- und Raumfahrt e. V.
Braunschweig, West Germany

Abstract

For the realization of flight tests not only advanced sensors are today at the engineer's disposal but also advanced data evaluation techniques. The application of both - hardware and software - opens new domains either for the accuracy of flight test reference systems or for the insight into complex systems to be flight-tested.

The sensors used during flight tests at DFVLR consist of groundbased sensors, i. e. tracking radar and/or cinetheodolites and of on-board sensors, i. e. inertial navigation system (INS), Doppler radar and barometric altimeter. All data recorded during flight are evaluated off-line using optimal filtering and smoothing algorithms.

The techniques described were applied for different tasks. During testing of the German microwave landing system DLS the accuracy of the reference flight path was at stake. The off-line optimal combination of the INS, radar and/or cinetheodolite data guaranteed the required accuracy which had not yet been achieved. A similar task was encountered during the testing of a Doppler radar system. Again the data of an INS were optimally combined off-line with radar data for setting up a reference velocity. In a third task the INS itself was flight-tested. The goal was to obtain a deeper insight into the system and the sensor errors. Again similar hardware and software combinations were used.

All three applications are discussed in the paper and test results are presented.

I. Introduction

The international efforts in the development of a Microwave Landing System (MLS) for the replacement of the present Instrument Landing System (ILS) are well known. Once it will be introduced the pilot or the automatic landing system will have available a continuous and accurate measurement for the position of the aircraft during landing and take-off on nearly any trajectory.

Specialists are discussing already the possibility, that this MLS will some day be surpassed by the Global Positioning System (GPS) which allows similar measurements not only in the vicinity of the airport, but worldwide.

Technology progresses also with the on-board instruments of an aircraft as with Doppler Radar (DR), Attitude and Heading Reference Systems (AHRS) and Inertial Navigation Systems (INS).

Along with the development of such navigation aids the engineer is forced to improve the reference systems for flight-testing new systems.

Additional requirements for accuracy improvements stem also from new measurement tasks on-board the aircraft. One knows already that some

aircraft crashes were due to shear winds during the approach phase and one believes that some crashes whose causes could not be found were also due to this effect. To avoid such tragedies shear winds should be measured on-board the aircraft, which from the technical standpoint means that airspeed and groundspeed as well as their time derivatives and local derivatives have to be determined on-line.

It will be shown in the following that advanced instrumentation in form of an INS on-board the aircraft and highly accurate position measurements from radars and cinetheodolites combined with advanced software in form of optimal filtering and smoothing techniques allow to meet the present measurement requirements. This statement will be proven by three examples, the testing of the German MLS which was the contribution in the ICAO contest, the testing of a Doppler radar and finally the testing of an INS. All activities were carried out at DFVLR in Braunschweig, Germany.

Before presenting the results, we will try to obtain an understanding for the central role the INS plays in such tests and for the software employed to combine the data from different sources.

II. The INS as Core of a Flight Test Reference System

The INS layed out during World War II in Germany /1, 2, 3/ was first viewed upon as an improved compass, indicating true north under any maneuver of the aircraft. It was brought into existence after the war primarily in the United States /3/.

An INS indicates true north with highest accuracy only if it is at the same time also aligned most accurately in the vertical and if in addition the north-south and the east-west velocities as well as the geographical latitude, i. e. the position with highest accuracy are known. Therefore in an autonomous INS a closed chain of information on

the north direction,

the vertical,

the over-ground velocities in north-south and east-west directions,

and

the position in geographical latitude and longitude

is implemented as hinted at in Figure 2.1.

As an INS has this information essential for flight guidance available in the form of a closed chain, it is not only an improved compass but doubtlessly nowadays the most attractive among the various navigational systems in civil and military aviation, in space flight, in sea navigation and for missiles.

Aside from navigation the INS is also increasingly used as a measuring instrument in flight tests and in all such cases when on a moving base measurements with respect to the vertical have to be carried out (e. g. surveying of railway tracks).

In order to explain the attractiveness of the INS as a flight test instrument let us have a look at the 1σ -errors in attitude, heading, ground speed and position of systems used in civil and military aircraft /4, 5/.

The sensor errors - accelerometer bias in the order of 10^{-4} g and gyro drift of $1/100$ °/h - cause misalignment errors of the platform in the self-alignment process prior to take-off and additional system errors en-route with the following short-time characteristics as shown in Figures 2.2a to c:

- in attitude an oscillatory motion with an amplitude of 0.5 min and a period of 84 min.;
- in heading approximately a constant misalignment error of 3.5 min;
- in ground speed an oscillatory motion with an amplitude of 1.2 m/s and a period of 84 min.;
- in position an oscillatory motion with a period of 84 minutes and an increasing mean whose slope is 1.2 km/h.

Figs. 2.3a to c confirm these simulation results. They show the acceleration, velocity and position errors of an experimental INS (Litton LN-3A platform with Honeywell H 316 computer).

The graphs just shown leave the impression that for many flight test applications these errors are tolerable. But since each error source, once it is known, causes a fairly predictable system error one should be able to estimate the error sources by a continuous measurement of the system position errors, for instance. The predictability of the INS system error for known sensor and misalignment errors can be traced in the INS error model shown in Figure 2.4 /5/. It is the physical explanation for the potential accuracy improvement of an INS "aided" on the position level with measurements from ground based sensors such as radars and cinetheodolites, for instance, shown in Figure 2.5.

With any new measurement in the position the difference can be computed between INS and radar position, which is fed into the optimal estimator which updates the precomputed INS error. In this updating process the incoming new information and the precomputed INS errors are weighed by the 1σ -values for the noise in the radar measurement and for the precomputed INS error shown in the preceding figures.

The uncertainty in the estimation of the INS error decreases with every incoming new information, i. e. the knowledge in the true heading and attitude of the aircraft, and in its ground speed and position increases, thus improving the conditions for flight test evaluation.

The updating philosophy we just described is widely described in the literature as Kalman filtering /6, 7/. It can be applied on-line once the data are available on board the aircraft. For flight testing the on-line data evaluation is often not required. It is sufficient to store the data and evaluate them off-line. This not only opens new possibilities for the use of sensors whose data need time for processing such as cinetheodolites, but also to apply even more powerful updating algorithms known as optimal smoothing /8, 9/. Figure 2.6 shows in principal the smoothing philosophy in form of the estimation accuracy over time for a Kalman filter working from the beginning of the test in the positive time direction and for another Kalman filter working from the end of the test in the negative time direction. From Figure 2.6 finally the accuracy improvement can be seen when the estimations of the forward and the backward filters are combined in a smoother. The forward filter gives for a time t_0 the optimal estimate based on all data before t_0 , the backward filter gives the optimal estimate based on all data after t_0 , and the forward/backward filter gives the optimal estimate based on all data before and after t_0 . In Figure 2.6 also the simple relationship for the accuracy gain of the smoothed estimate as compared to that of a forward and a backward filter estimate is mentioned.

Between t_1 and t_2 in Figure 2.6 it is assumed that the INS navigates unaided with the 1σ -band growing according to the unaided error model (s. Figure 2.2c) for the forward and the backward filters. The smoothed estimate bridges the time with much smaller loss in accuracy. This proves that for the off-line flight test data evaluation the smoothing algorithms are suited best. Not only is the 1σ -band smoother than that of the Kalman filter, but also the estimate itself because the forward filter estimate is much more sensitive to stray points in the measurements /10/.

In practice one applies the Kalman filter algorithms forward in time, and when the end time is reached, the Rauch-Tung-Striebel or Fraser algorithms backward in time /8, 9/.

We will see in the following how the instruments and the software were applied in three major projects carried out at DFVLR in Braunschweig, Germany.

III. Testing of the Microwave Landing System DLS

As already mentioned above the DME-based Landing System (DLS) has been the German candidate in the ICAO competition for the next generation landing systems. The DLS has been tested by DFVLR at the airport of Braunschweig. The whole potential of the data evaluation and measuring techniques mentioned above had to be utilized for bringing the test to a success. We will concentrate in the following only on the main aspects of this project. A more detailed discussion can be found in /10/.

The DLS landing system had to be tested mainly in-flight, so that the outputs of the DLS-on-board sensors could be compared with respect to a reference flight path. The accuracy requirement for the reference flight path defines the sensors in-

tegrated in the tracking system. According to a rule of thumb, the requirements should be better by one order of magnitude, which could be met only if at least for short ranges the measurements were based on cinetheodolites. They are up to now the most accurate tracking sensors. The cinetheodolites have one drawback: the data evaluation is cumbersome, especially if it is done by hand and can only be carried out off-line. In order to alleviate this problem DFVLR had decided to pursue the following proposal (s. Figure 3.1).

The ground based sensors, i. e.

3 cinetheodolites,
1 tracking radar

giving intermittent tracking data with high accuracy were supplemented by on-board sensors, i. e.

1 inertial navigation system,
1 barometric altimeter

giving continuous tracking data. It was the task of the altimeter to aid the INS in the vertical channel.

As shown in Figure 2.2c the INS has high short time but inferior long time accuracy. Thus the characteristics of ground-based and on-board sensors are complementary as it is required for the off-line optimal INS error estimation process.

For carrying out the measurements it was necessary to define a rectangular coordinate system. The origin of this system was centered in the azimuth antenna of the DLS system (DLS-A-Station). The x-axis was aligned with the runway and pointed nearly east (84.782°), the y-axis nearly north and the z-axis upwards.

The on-line data flow in Figure 3.1 is the following. The time base of the system was a digital counter (frame counter) on board of the aircraft. By means of a PCM telemetry system the following data required for the computation of the flight path were transmitted to the ground with a frequency of 30.518 Hz:

frame counter setting,
3 accelerations as measured by the inertial platform,
2 velocities as computed by the analog computer of the inertial system,
roll, pitch, and yaw angles of the aircraft,
barometric altitude.

The setting of the frame counter received on ground, controlled the radar and cinetheodolite measurements. This guaranteed a high accuracy for the synchronism of all data measured on ground and on board. The time between 2 fixes was in general 8,388 s. The radar measurements were plotted on-line and also stored on punch tape.

The cinetheodolites are of the type KTH 59 and made by Bodenseewerk. Here the tracking is done manually by handwheels and by means of telescopes. During the DLS trials, one registration was made approximately every eight seconds.

The tracking radar was of the type L 4/3 and made by Hollands Signaalapparaten. This radar fol-

lows the target automatically during the measuring process, and gives the angle of elevation and the azimuth of the antenna system, apart from the slant range of the target itself. Automatic tracking is achieved by rotating of the radar beam (conical scan). The distance of the target is determined by the interval between transmission and reception of every individual radar pulse.

The test aircraft Dornier Do 28 is shown in Figure 3.2. As reference point for the cinetheodolite measurements, a flash lamp at the aircraft was used mounted between the main landing gears. Since the flash light is not visible on every cinetheodolite picture, the measuring accuracy of the cinetheodolites was limited to 0.3 m for the error analysis.

Part of the on-board electronics can be seen in Figure 3.3: The inertial system (Litton LN3-2A) and the CAMAC interface for digitizing the signals and feeding them to the PCM telemetry. Not included in the figure is the barometric altimeter Model 840E of the Rosemount Engineering Company, USA.

The inertial system consists of the inertial platform, the analog computer, the flux valve for coarse alignment of the platform and the align control plus switch-in unit. This unit contains also the preamplifier and analog readout for the signals.

In general, only three measurements are necessary to determine the position of a target. Out of the three cinetheodolites and the tracking radar nine measurements are available and the position of the target is overdetermined. Therefore the calculation of the various position fixes was achieved by means of an optimum fitting according to the method of least square errors. The evaluation program for the computer was set up in such a way as to permit also working with less than nine data. For further processing, the coordinates of the position fixes were stored on magnetic tape. The accuracy of the various points has to be expressed by the error covariance matrix as a necessary input information for the optimal estimation process in the computer. It was determined for each position fix and was also stored on the magnetic tape.

Based on the INS velocity outputs the computation of the raw flightpath was carried out with a frequency of 5 Hz. By comparison of the frame counter setting on the magnetic disc and on the magnetic tape a position fix was recognized by the computer which started the forward Kalman filter algorithm (s. Section 2) for estimating the INS error state vector. The state vector, state transition matrix, covariance matrices before and after the measurement were temporarily stored on magnetic disc. If the end time (last position fix) was at hand, the smoothing of the INS errors (using the Rauch-Tung-Striebel algorithms (s. Section 2)) backward in time was started based on the parameters just mentioned.

Since final smoothed error state vector estimations for correcting the INS flightpath are 8 seconds and sometimes more apart (if no position fix was at hand), but the flightpath had to be corrected at a frequency of 5 Hz, the errors between the

8 seconds had to be calculated by interpolation. Then the final reference flightpath could be calculated. Since the optimal estimation was not tied down to fixed time intervals, the reference flightpath computation could also be carried out when the aircraft was out of the ranges of the tracking radar and the cinetheodolites. The reference flightpath was then based solely on the INS with position errors growing according to its dynamics.

In the following, the accuracy of the reference trajectory in form of the 2σ -bands, is described, which were achieved in three typical flight tests in the way just described. These 2σ -bands for the reference flightpath is simply twice the square root of the corresponding value on the main diagonal of the covariance matrix which is computed by the optimal filtering and smoothing algorithms on-line for self-diagnosis. In these cases the errors were computed with respect to the DLS-coordinates, azimuth, elevation and slant range.

In Figure 3.4 to 3.6 the aircraft was flying at 10,000 ft from 32 nm to 2 nm on a radial towards the DLS-A station. Because of insufficient visibility, no cinetheodolite measurements were possible. The reference trajectory was computed using the tracking radar and INS data. The maximum range of the radar is 28 nm; therefore beyond 28 nm, only INS is available, which leads to relatively large errors of the reference trajectory. This is clearly to be seen in the plot for the DME error. The effect is almost not visible in the plots for the angular errors because with increasing x, y and z-errors also the distance to the origin of the coordinate system (DLS-A-Station) is large. The angular errors are increasing in the plots due to the inverse geometrical effect when the aircraft approaches the DLS Stations.

In Figure 3.7 the aircraft was flying at 3,000 ft on a radial to the DLS-A station. This flight illustrates the reference trajectory accuracy, when different combinations of the sensors are used: Beyond 9 nm tracking radar and INS is available. For a short period of time the radar had lost the target. Between 9 and 5 nm, only one cinetheodolite could track the aircraft. At a distance of 1 nm from the DLS-A station - i. e. close to the DLS-E station - a telemetry break-down occurred, because the aircraft was flying overhead the telemetry station. So the synchronization was cut off and no on-board data were available for the evaluation.

Figure 3.8 displays the errors for a final approach. In this case all sensors were in operation (3 cinetheodolites, tracking radar and INS). The geometrical effects due to small distance between the aircraft and the DLS stations are clearly visible.

Figure 3.9 shows the results of the measurements taken during a conventional centerline approach. In the Figure the difference between the y-components of the DLS-signal and the reference is displayed in rectangular coordinates. The reference trajectory in this case has been calculated by smoothing the cinetheodolite data with the INS.

The mean value of this difference is very small, 0.42 m. The standard deviation (1σ) is also very small, as can be seen in this Figure, i. e. 0.75m. The error of the reference system is certainly not correlated with the DLS error, so that the assumption is correct, that the random error of the reference (1σ) is not greater than 0.75 m. But the structure of the difference signal clearly indicates that the main part of this error is due to the DLS system, because the reference trajectory cannot contain such high frequency errors. The conclusion can be drawn, that the integrated reference system can provide an accuracy of the order of 50 cm, with cinetheodolite measurements taken every 8 seconds.

The overall results which have been obtained during the DLS testing campaign have shown, that the approach of an integrated measuring system for the flight path consisting of an INS and ground-based sensors combined by optimal smoothing techniques is economical with respect to the evaluation work load and provides very high accuracies.

IV. Testing of a Doppler Navigation System

The flight testing of Doppler navigation systems is another example of the successful application of a hybrid flight test reference system. We will summarize in this Section the flight test results described more in detail in /11/.

For the Doppler navigation system tests the DFVLR test aircraft HFB 320 (Figure 4.1) had been used. This aircraft contains advanced on-board instrumentation (Figure 4.2):

- fly-by-wire system
- general purpose on-board computer
- INS
- magnetic tape with high storage capacity
- quick-look capability
- different attitude reference systems etc.

For the Doppler tests as main on-board instruments the Litton LN3-2A inertial platform, the Sperry SYP-820 attitude and heading reference system (fabricated by Bodenseewerk, Germany) and three different types of Doppler radars (stabilized and fixed antennas, pulse and CW Dopplers) had been used. The measurements of these sensors were registered on the magnetic tape at high frequency (10 times per second).

As a typical example of a flight profile for long range tests, Figure 4.3 displays a flight from Hannover airport, via Meppen, Norderney and Helgoland back to Hannover. The flight track lies partly within the coverage range of three tracking radars, at Hannover (L 4/3), Meppen (MPS-36) and Norderney (Fledermaus). If available, radar measurements were also registered every 10 seconds and stored on magnetic tapes.

The time synchronization of the on-board and the ground based sensors was done off line with the aid of a time code which was also recorded on the magnetic tapes.

The error of a Doppler radar signal is illustrated in the Figure 4.4: The predominant error is the Doppler fluctuation, which can be observed

clearly in this Figure in comparison with the very smooth reference velocity. Velocity scale factor error and heading error are also contained in the Doppler navigation system error model.

The reference system for the Doppler navigation system testing was implemented in the same manner as described in Section 3. The accuracy of this reference system is illustrated by Figures 4.5 - 4.8. The Figures show the 1σ -bands for the accuracy obtained by forward Kalman filtering and by backward smoothing. The improvement introduced by optimal smoothing is clearly visible. When the aircraft flies out of the radar coverage, the errors of velocity and position increase, as can be observed in Figure 4.5 and 4.6. This increase is much less for the smoothing algorithms because the "gaps" between two radar coverages are closed from both sides as already indicated in Figure 2.6. Under tracking radar coverage the roll and pitch angles were estimated with a 1σ -accuracy of $10''$, the heading with $1.5'$, the velocity with 0.03 m/s and the position with $2 - 8$ m by the hybrid reference system. Figure 4.7 shows the difference between the reference trajectory and the radar measurements (curve 1). The 1σ accuracies of the tracking radars (curve 2) and the reference trajectory (curve 3) are also shown. This Figure demonstrates, the the measurements of the three tracking radars

- L4/3
- MPS-36
- Fledermaus

have approximatively the same error dynamics. This can be explained by the fact that these errors are mainly caused by the radar fluctuations on the test aircraft HFB 320.

It has also been analyzed, what accuracy could be obtained, if instead of the INS, the Doppler radar plus heading reference (SYP 820) would have been taken to smooth the tracking radar data. This can be seen from Figure 4.8. It gives a comparison of the position measuring accuracy (smoothed estimates) of the two reference systems

- INS and tracking radar,
- Doppler plus heading reference and tracking radar

for the long range flight shown in Figure 4.3. This Figure shows the higher accuracy obtained with the INS under radar coverage in comparison with the Doppler system. Outside the radar coverage both systems have similar errors. In long periods between radar coverage the reference system with a Doppler plus heading reference of inertial quality has a higher accuracy than with an INS (in Figure 4.8 between 4500 and 5500 s).

As examples of the flight test results the Figures 4.9 - 4.11 are shown. Figure 4.9 shows the difference between the Doppler radar measurement and the reference velocity for a flight period of 90 s. This is part of the sample function measured in a flight over flat land. The mean value of this sample function has been computed over 200 s, which corresponds to a distance flown of 12 nm at 110 m/s. The mean value of the sample function was 0.067 m/s, which is negligibly small. The standard deviation of this sample function is $\sigma = 2$ m/s, a

value which is by several orders of magnitude greater than the reference velocity accuracy, so that it can be stated that this error is due to the Doppler radar measurement only. The sample function has been analyzed by computing its autocorrelation function.

Another sample function had been taken over water. Figure 4.10 shows the difference between the Doppler radar measurement and the reference velocity for 90 s flight time. The same analysis had been carried out for this sample function showing a mean error of 2.2 m/s and a standard deviation $\sigma = 1.4$ m/s. The corresponding autocorrelation function is shown in Figure 4.11. Near the origin an exponential decay can be observed showing a correlation time of 0.3 s. The large mean error in the sample function is due to the land/sea calibration shift. The sample functions show that the fluctuation error over sea has smaller amplitudes than over land. The statements made so far refer to the velocity measured in the aircraft's longitudinal axis. Similar results were obtained for the cross velocity.

In summary it can be stated that the Doppler errors observed in the flight tests are

- fluctuation error, exponentially correlated with a correlation time of a few seconds, and
- calibration shift error, due to land/sea shift, and
- calibration error, which was very small for the flight-tested Doppler radars, because this equipment had been very well calibrated prior to flights.

The calibration shift caused by variations of the backscattering properties between land and water has been found to cause an error of 2% of the velocity.

V. Testing of an Inertial Navigation System

In a third project the INS (Litton LN-3A) itself was at stake. This Section summarizes the test results described more in detail in /12/. The flight tests were carried out in the middle of 1976 on the HFB 320 shown in Figure 4.1. The following installations were used for the test: the INS to be tested, the altimeter (Conrac), the CA-MAC interface crate for connecting the instruments to the Honeywell DDP 516 computer, the on-board clock (Patek Philippe) and the digital magnetic tape recorder (Ampex ATM 13591 II) for recording all essential on-board data.

Tests were carried out from Braunschweig towards west and north.

On the westerly flight to Bedford, UK, the following tracking facilities were used, as shown in Figure 5.1:

Braunschweig (DFVLR)
1 tracking radar (1σ -accuracy in angle 0.05° , in range 8 m)

Meppen (Erprobungsstelle 61 der Bundeswehr)
1 tracking radar (1σ -accuracy in angle 0.025° , in range 2.7 m)

Amsterdam (National Lucht- en Ruimtevaartlaboratorium)

1 terminal approach radar (1σ -accuracy in horizontal position 200 m)

Bedford, UK (Royal Aircraft Establishment)

2 cinetheodolites (1σ -accuracy in angle 0.025°).

On the northerly flight to Oslo, Norway, the tracking facilities were those of Braunschweig and of

Oslo (Directorate of Civil Aviation)

1 terminal approach radar (1σ -accuracy 1 NM).

Valuable position and velocity measurements were yielded also when the aircraft was stationary on a reference point before take-off and after landing.

The second aircraft shown in Figure 5.1 served as a relais plane, for the long-distance transmission of the measurement data in the HFB 320 to Braunschweig where they could be recorded on-line for the purpose of quick-look.

In the following we will concentrate on the test results of the flight from Bedford back to Braunschweig.

All data on-board (INS, altimeter) and on ground (radar, cinetheodolites) were recorded synchronously. From the ground measurements the position of the aircraft in geographic longitude, latitude and altitude had to be calculated as well as the covariance matrix based on the above mentioned sensor specifications /10/.

Figure 5.2 shows the plot of the flightpath with the crosses indicating the city of Bedford (UK), Amsterdam, Meppen (Ger) and Braunschweig. The aircraft carried out maneuvers in the range of each radar/cinetheodolite station in order to improve the observability of the INS errors.

The following discussion shall be based on the test results for the north-south and the azimuth channels only.

If all available position fixes and stationary measurements are combined with the INS data by means of smoothing algorithms, the accuracy of the reference flightpath is better than 45 m according to the self-diagnosis of the forward/backward filter, s. Figure 5.3. The highest value is at 1/2 h elapsed time when the aircraft is above the North Sea. The position differences (reference flightpath minus position fix) are well distributed about the center line of the plot, indicating that the results are reasonable.

In Figure 5.4 the results for the INS geographic latitude error estimation are plotted. The 1σ -band corresponding to the 45 m maximum mentioned above is indistinguishable on the plot. The smoothing algorithms estimate a linearly increasing error due to azimuth misalignment and vertical gyro drift (cross track error).

Figure 5.5 shows the corresponding results for the north velocity error estimation. The 1σ -band

is $< 0,1$ m/s. The estimation shows a Schuler oscillation with spikes superposed. Due to the cross track error, the spikes are correlated with turns of the aircraft.

In Figure 5.6 the results for the east-west misalignment are plotted. The smoother's self diagnosis is at ± 1.1 sec. The estimation of the misalignment error shows Schuler oscillations.

Figure 5.7 shows us that the east-west gyro drift can very well be calibrated on a maneuvering vehicle. The 1σ -band is at $\pm 5 \cdot 10^{-3}$ $^\circ$ /h, the mean estimate is approximately at $3 \cdot 10^{-2}$ $^\circ$ /h with a change of approximately $-5 \cdot 10^{-3}$ $^\circ$ /h.

In Figure 5.8 the results for the azimuth alignment error are plotted. According to the 1σ -band the error estimate is better than 2 min. The initial misalignment error in Bedford, UK, was according to this plot -0.5° , changing linearly with time according to the azimuth gyro drift of -0.27 $^\circ$ /h. The final alignment error is approximately -1° when the aircraft lands in Braunschweig. These results prove that for this particular INS unit

- the initial misalignment error and
- the azimuth gyro drift

by far exceed the requirements for an operational system. The flight tests described in this paper had been carried out with an uncalibrated LN-3A system in which essential parts of the computer had been exchanged.

The results presented do not yet reflect the final state of the research. Topics for the continuation of the efforts are the improvement of the INS- and its sensor error models based on more flight test experience.

VI. Summary

Accuracy improvements for flight test reference systems are achievable only if hardware and software improvements go hand in hand. The present state of the art at DFVLR has been exemplified with three projects, the testing of an MLS, a Doppler radar system and an INS. It was shown that the reference system accuracy was adequate for the measurement requirements. Better instrumentation, i. e. the use of better INS equipment and improvements in the modelling of its sensor errors will open the way for pushing technical accuracy limitations further aside.

References

- /1/ Gievers, J. "Erinnerungen an Kreiselgerä-
te",
Jahrbuch 1971 der DGLR, Seite
263 - 291.
- /2/ Sorg, H. "From Serson to Draper, Two
Centuries of Gyroscopic Deve-
lopment",
Proceedings of the Internatio-
nal Navigational Congress 1976,
page 166 to 172.

- /3/ Wrigley, W. "History of Inertial Navigation", Proceedings of the International Navigational Congress 1976, page 92 to 95.
- /4/ Britting, K. "Inertial Navigation System Analysis", Wiley Interscience, 1971.
- /5/ Stieler, B. "Einführung in die Trägheitsnavigation", Deutsche Forschungs- und Versuchsanstalt für Luft- und Raumfahrt e. V., Interner Bericht IB 153 - 76/28, 1976.
- /6/ Gelb, A. "Applied Optimal Estimation", The MIT Press, 1974.
- /7/ Schrick, K. "Anwendung der Kalman-Filter-Technik, Anleitung und Beispiele", Oldenbourg Verlag, 1977.
- /8/ Rauch, H.E. "Maximum Likelihood Estimates of Linear Dynamic Systems", AIAA Journal, Vol. 3, No. 8, 1965, Seite 1445.
- /9/ Fraser, D.C. "A new Techniques for the Optimal Smoothing of Data", MIT Doctoral Thesis, T 474, 1967.
- /10/ Hurraß, K.H. Stieler, B. "Zum Einsatz des hybriden Flugmeßsystems bei der Vermessung eines Mikrowellen-Landesystems", Proceedings of the Symposium Kreisellechnik 1976 of Deutsche Gesellschaft für Ortung und Navigation, Düsseldorf, page 305 to 328.
- /11/ Benecke, W. Dombrowsky, R. "Ergebnisse der Flugerprobung von Dopplerradargeräten", Deutsche Forschungs- und Versuchsanstalt für Luft- und Raumfahrt e. V., Interner Bericht IB 153 - 76/14, 1976.
- /12/ Stieler, B. Lechner, W. "Calibration of an INS Based on Flight Data", Proceedings No. 220 of the AGARD Conference Applications of Advances in Navigation to Guidance and Control, Stuttgart, 1977, page 5-1 to 5-14.

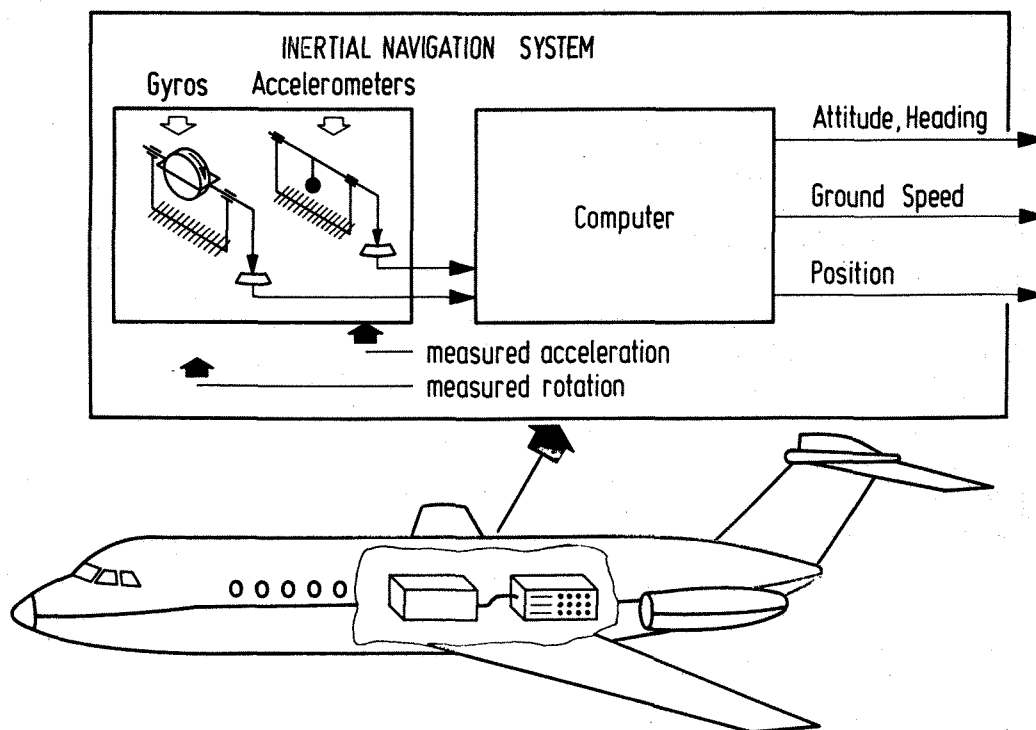
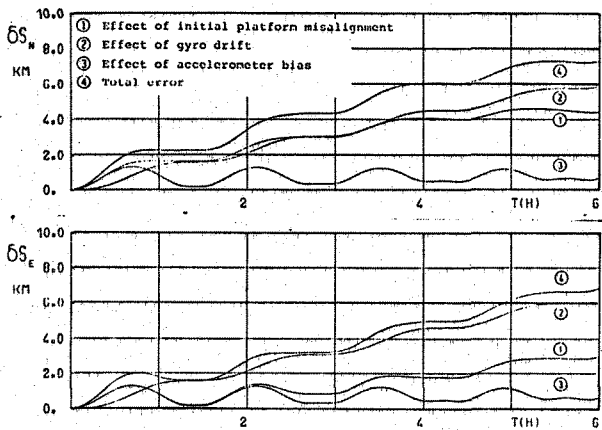
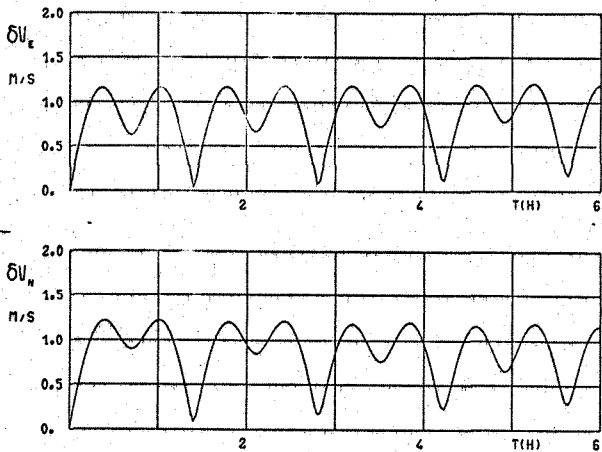
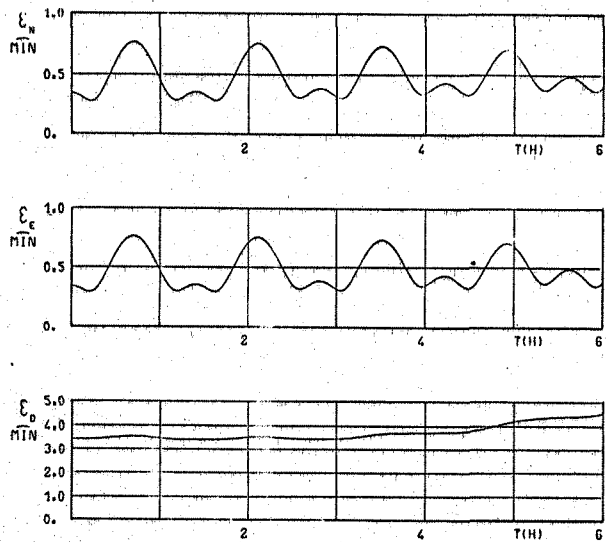


Figure 2.1 The INS as Reference System for Attitude, Heading, Groundspeed and Position



Velocity: $V = 0$
 Initial misalignment angles: $\epsilon_N = \epsilon_E = 0.1 \text{ mrad} = 0.34 \text{ mIN}$
 $\epsilon_D = 1 \text{ mrad} = 3.4 \text{ mIN}$
 Gyro drift: $D_N = D_E = D_D = 0.01 \text{ }^\circ/\text{h}$
 Accelerometer bias: $B_N = B_E = 0.0001 \text{ g}$

Figure 2.2 1σ - Errors for INS Attitude ($\epsilon_{N,E}$), Heading (ϵ_D), Velocity ($\delta V_{N,E}$) and Position ($\delta S_{N,E}$)

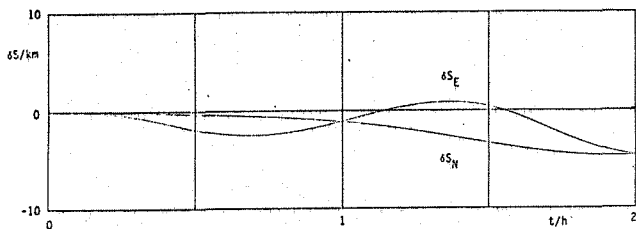
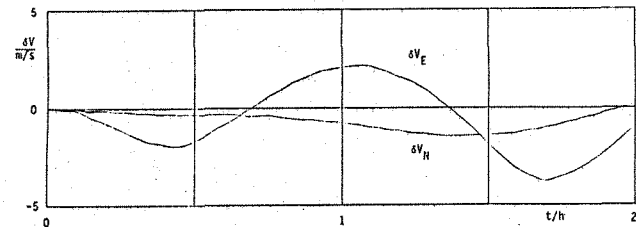
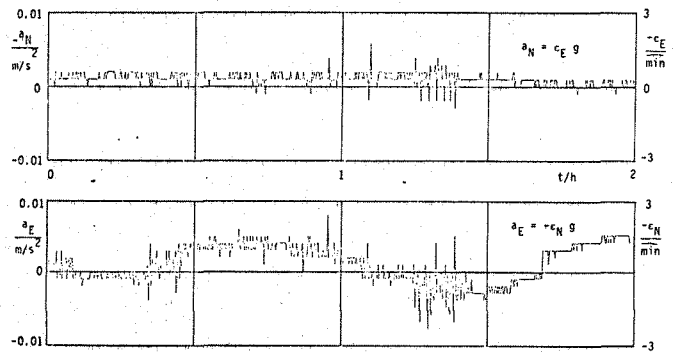


Figure 2.3 Errors in Acceleration ($a_{N,E}$), Velocity ($\delta V_{N,E}$) and Position ($\delta S_{N,E}$) of a Litton LN-3A INS During a Stationary Run

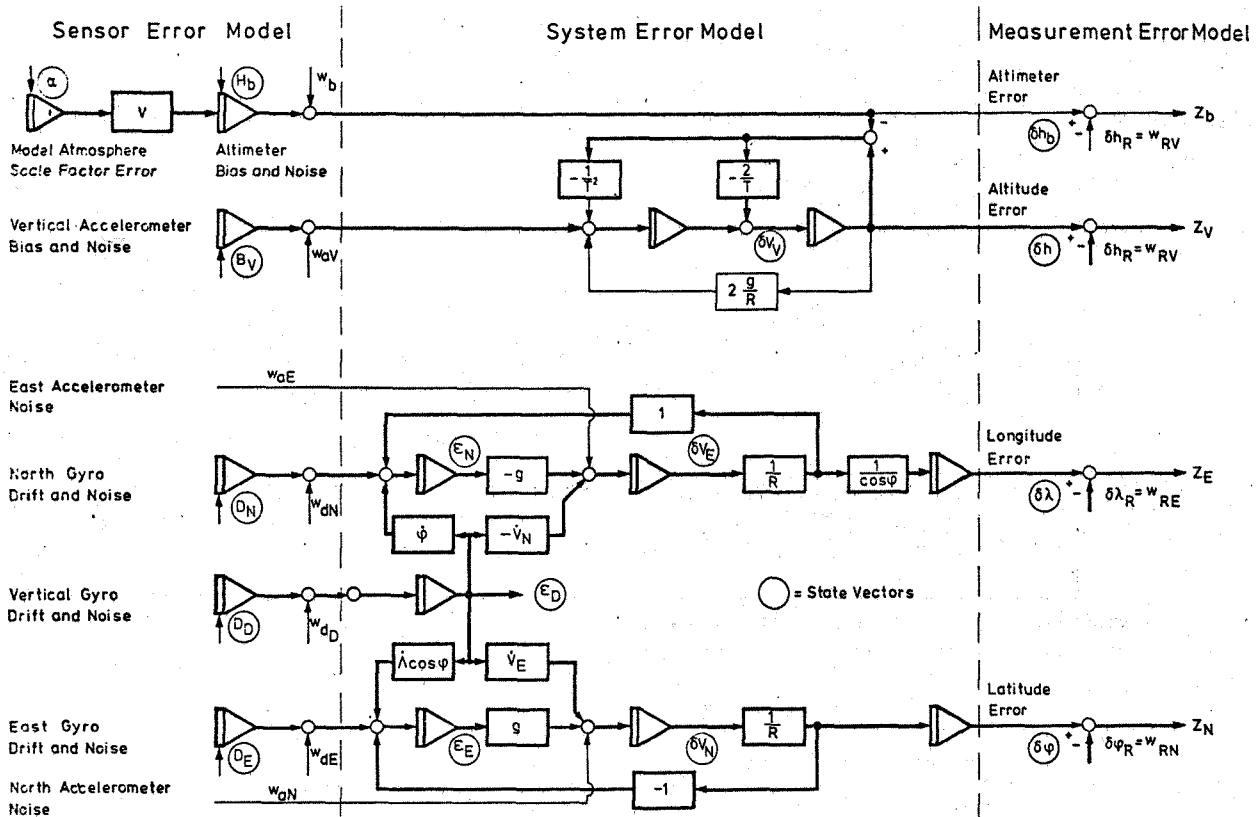


Figure 2.4 Error Model for the INS, Barometrically Aided in the Vertical Channel and for the External Position Measurements

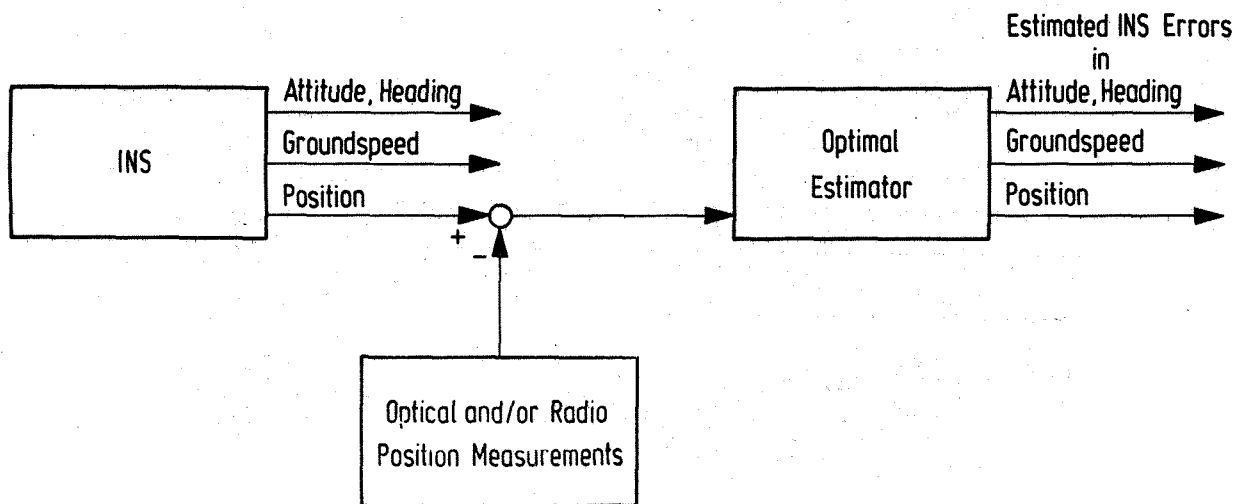


Figure 2.5 Block Diagram for the Aiding of the INS by External Position Measurements

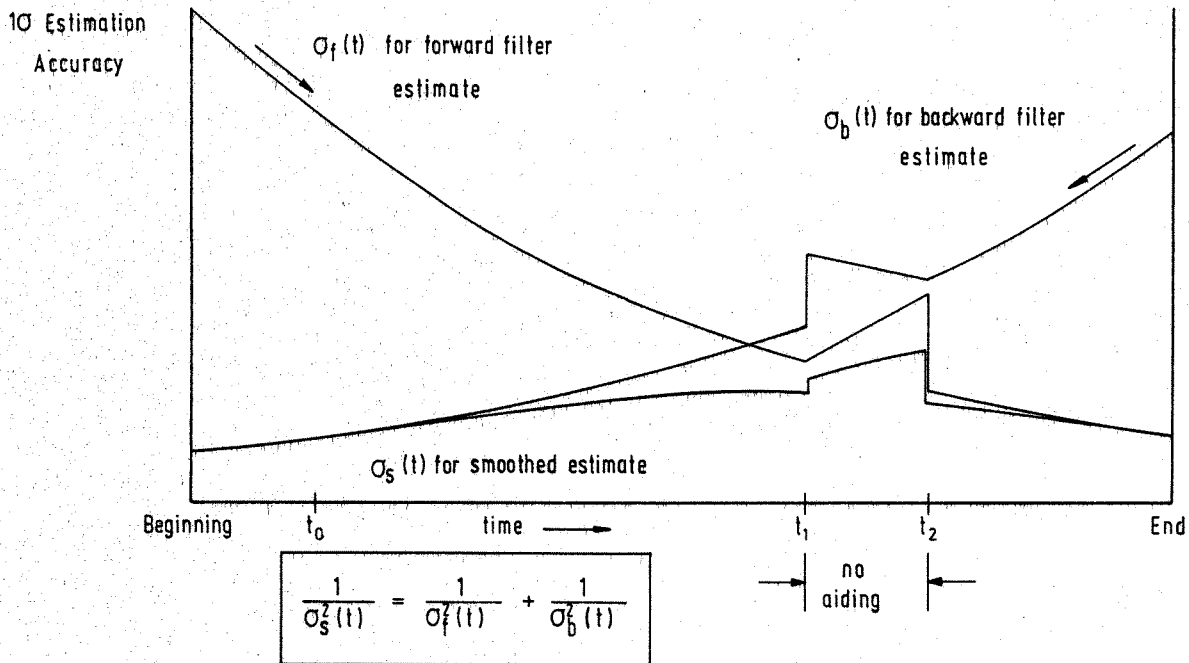


Figure 2.6 Aided INS 1σ - Estimation Accuracy with Forward Filter, Backward Filter and Forward / Backward Filter (Smoother)

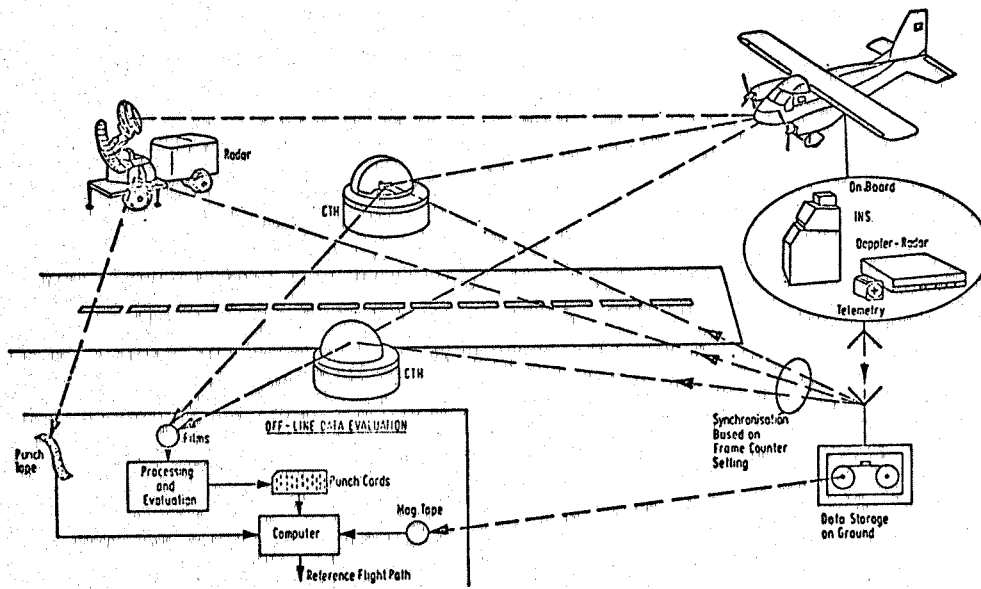


Figure 3.1 Hybrid Measurement System for Testing the DLS Landing System

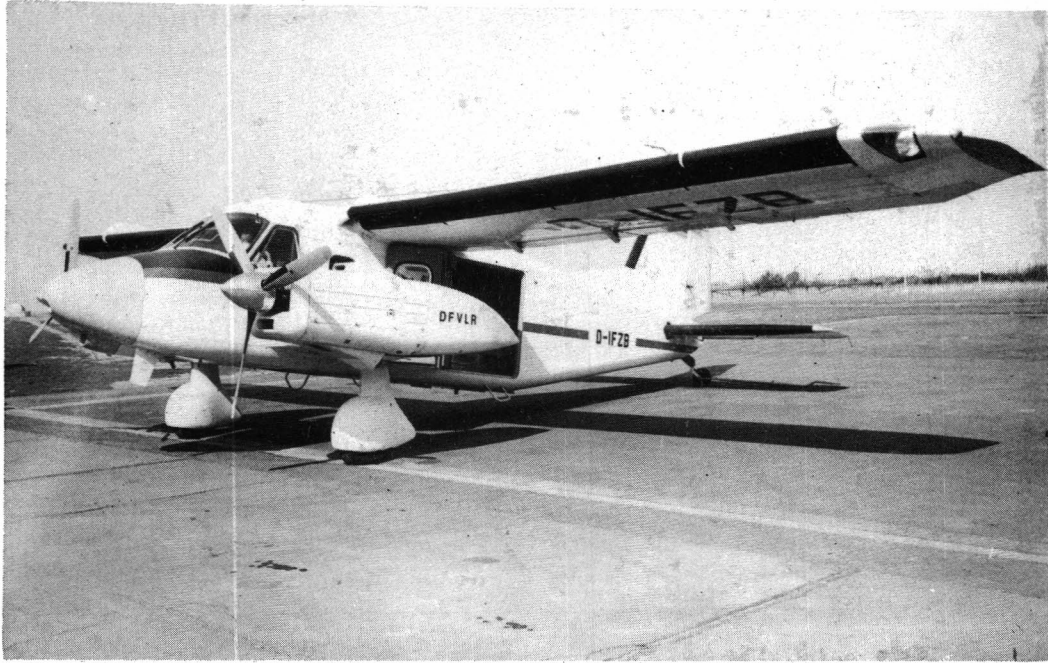


Figure 3.2 Dornier Do 28 Test Aircraft of DFVLR

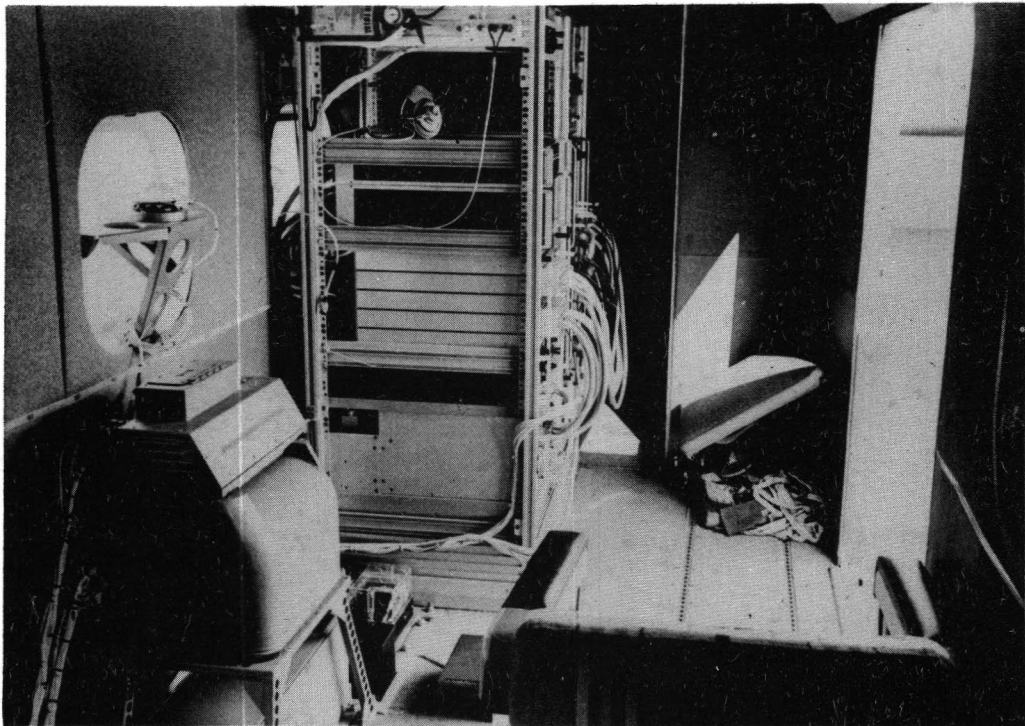


Figure 3.3 The On-Board Electronics in the Do 28

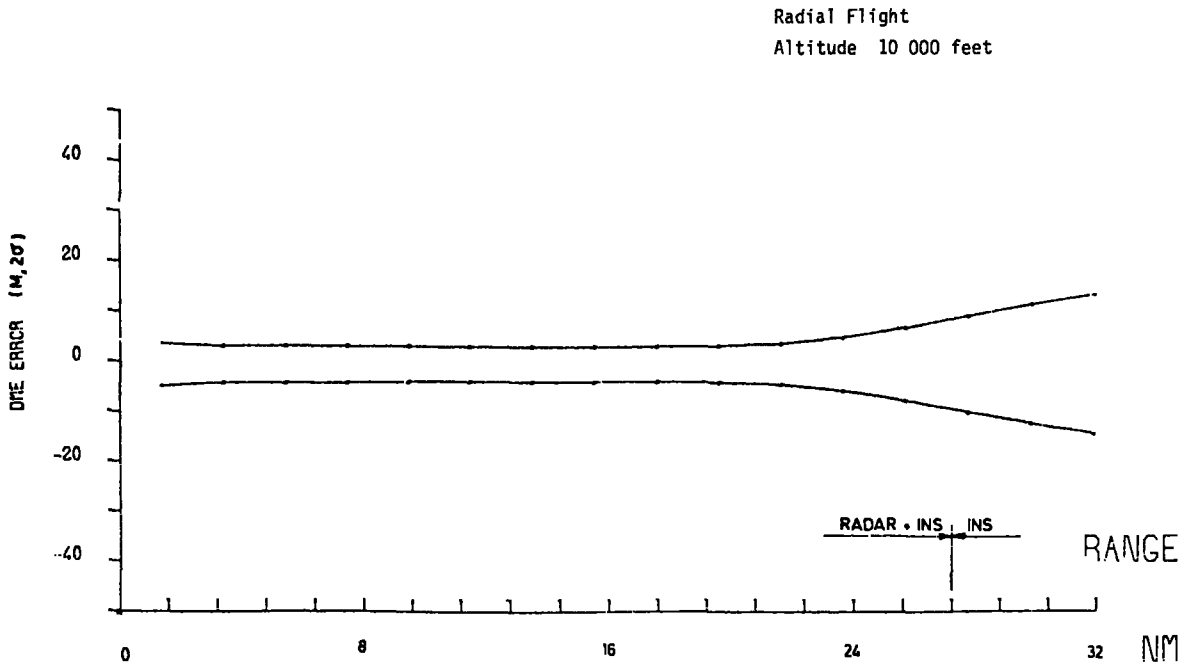


Fig. B6-1

Figure 3.4 2σ - DME Accuracy Bands of the Reference Flight Path for an Inbound Radial Flight (radar plus INS only).

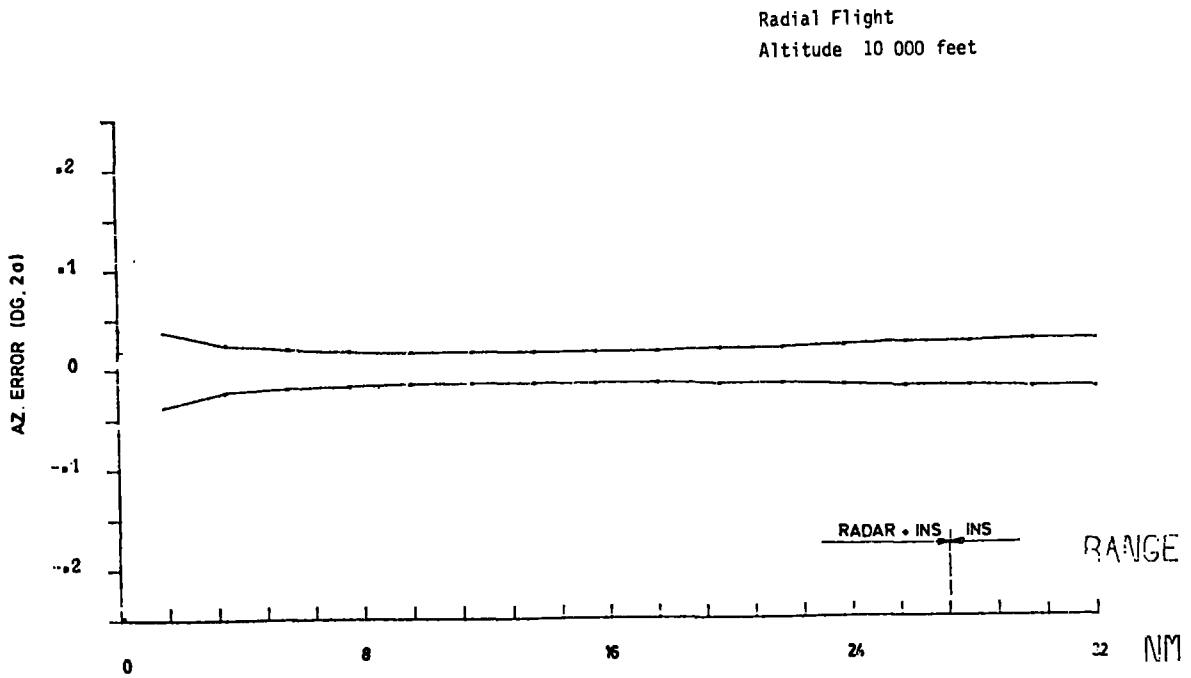


Fig. B6-2

Figure 3.5 2σ - Azimuth Accuracy Bands of the Reference Flight Path for an Inbound Radial Flight (radar plus INS only).

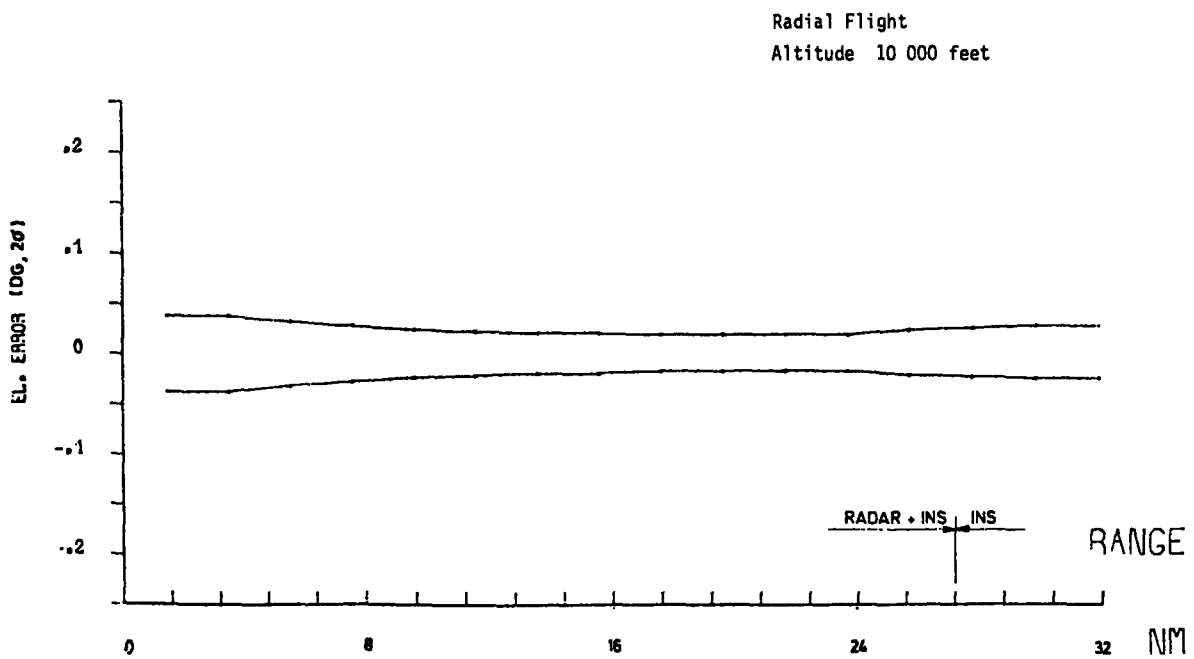


Fig. B6-3

Figure 3.6 2σ - Elevation Accuracy Bands of the Reference Flight Path for an Inbound Radial Flight (radar plus INS only).

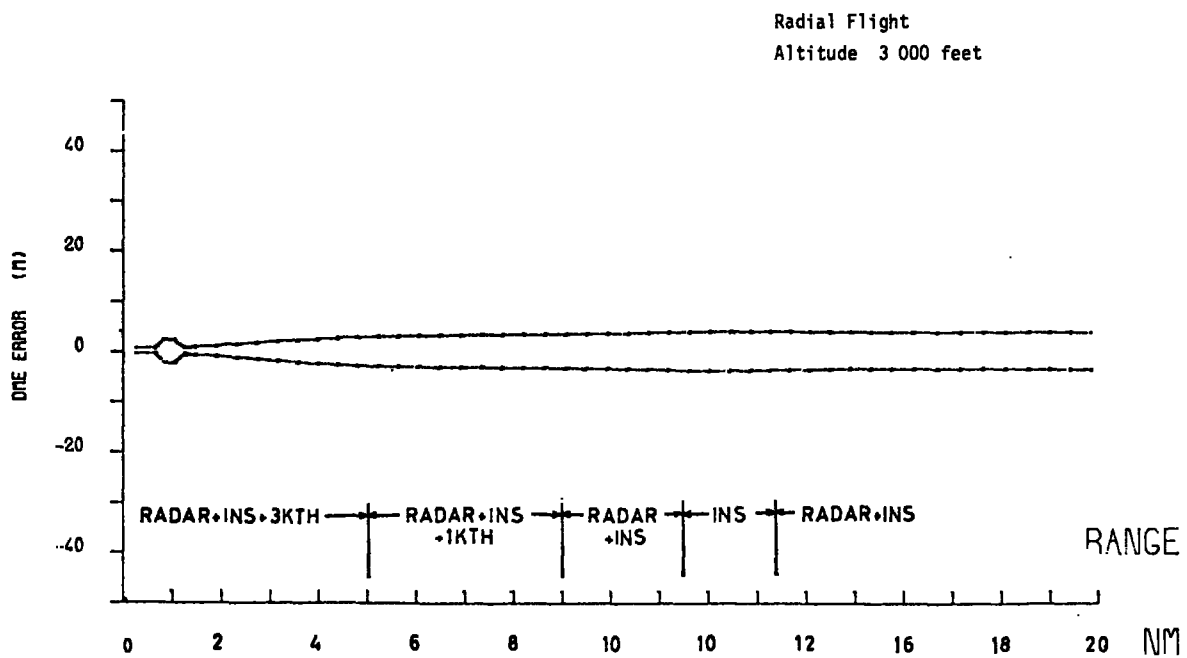


Fig. B6-4

Figure 3.7 2σ - DME Accuracy Bands of the Reference Flight Path for an Inbound Radial Flight (different sensor combinations).

Conventional Centerline Approach
Glide Slope 3 degrs.

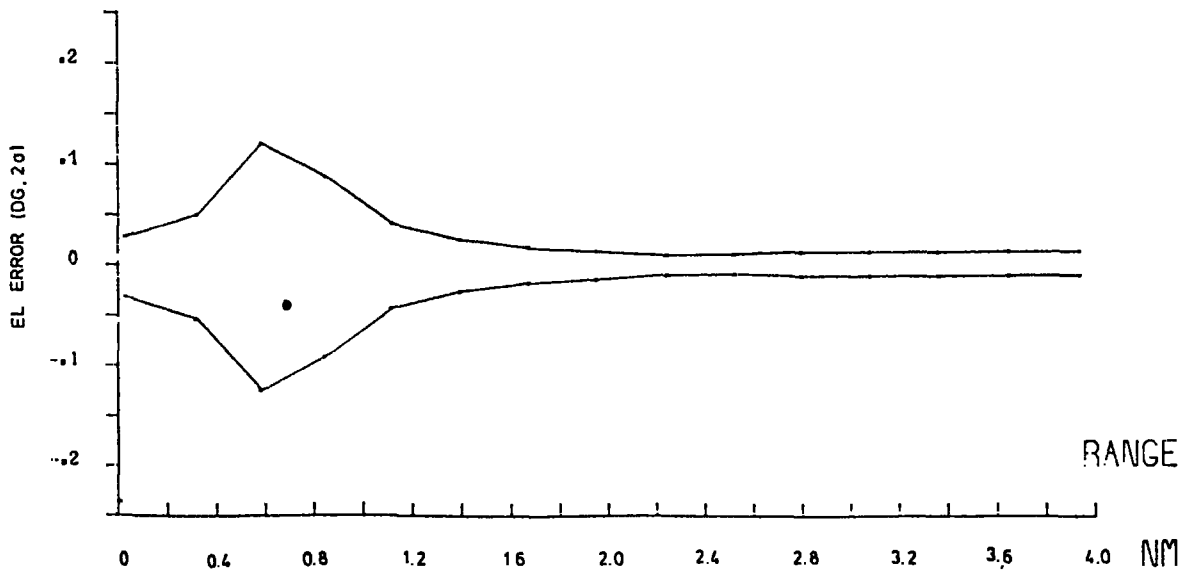


Fig. B6-9

Figure 3.8 2σ - Elevation Accuracy Bands of the Reference Flight Path for a Final Approach (3 CTH, radar plus INS).

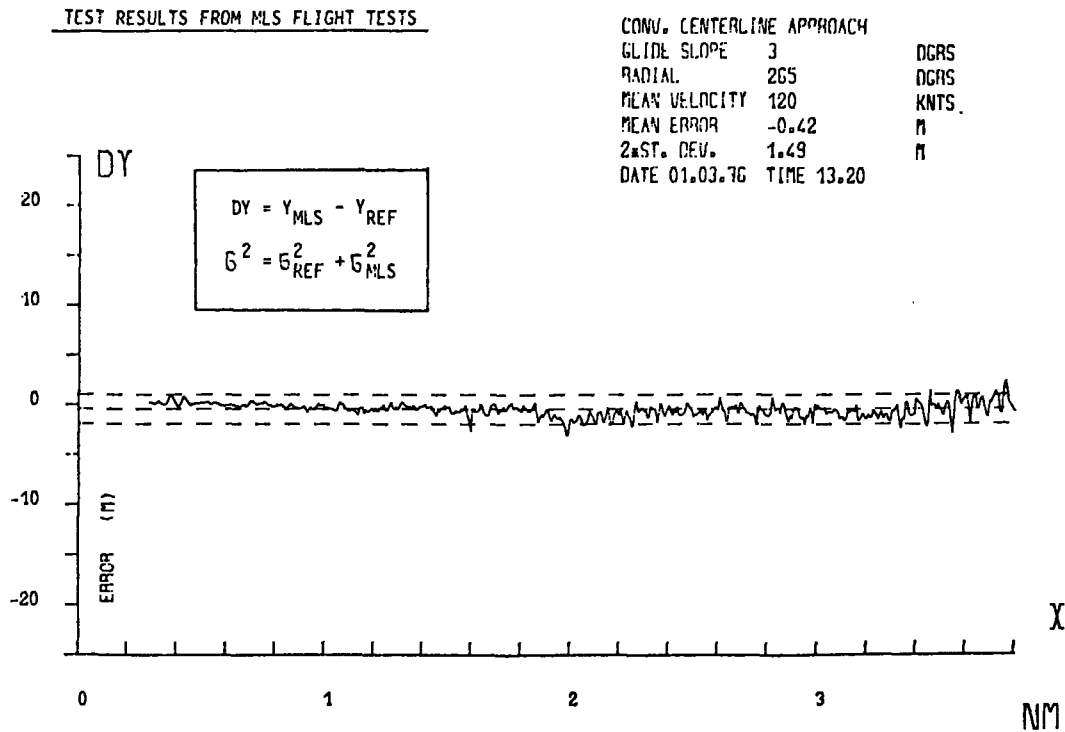


Figure 3.9 Cross-Track Difference between DLS and Reference Flight Path (3 CTH plus INS)



Figure 4.1 DFVLR Test Aircraft HFB 320

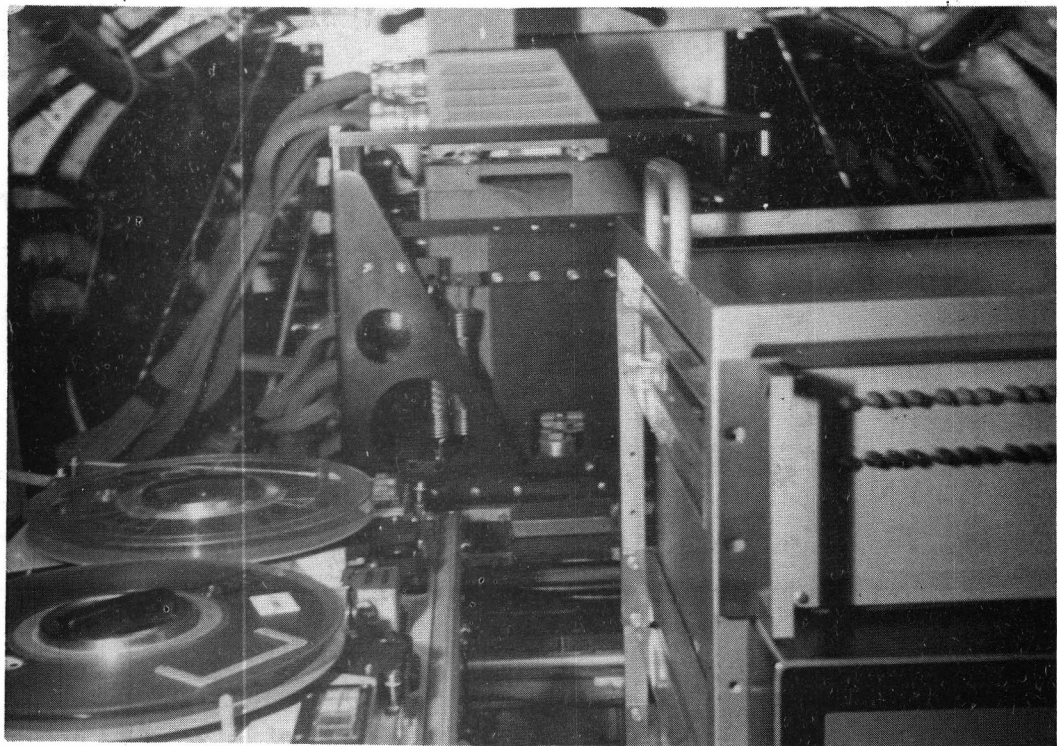


Figure 4.2 The On-Board Electronics in the HFB 320

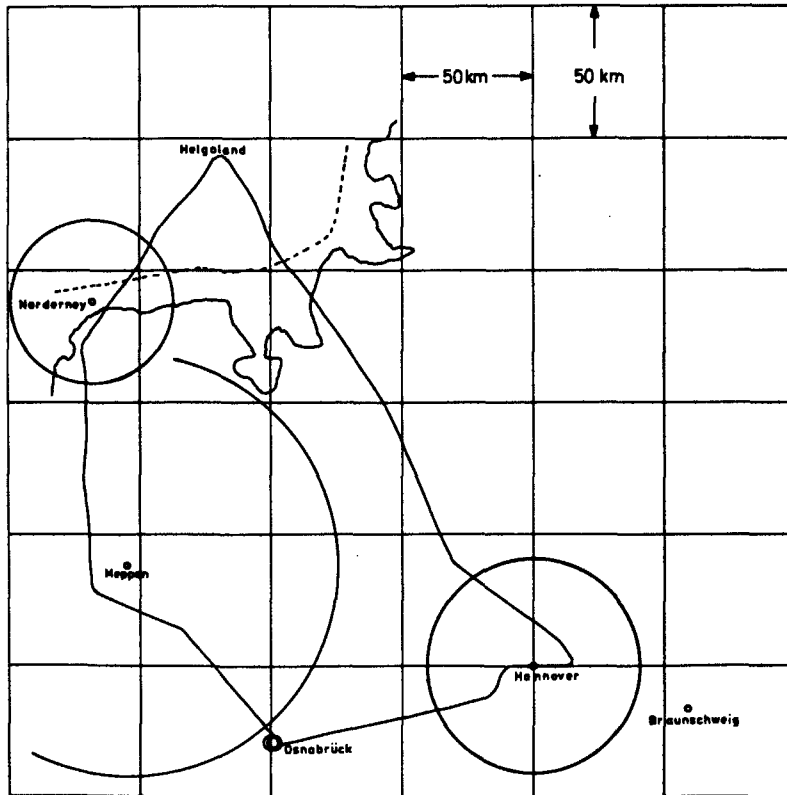


Figure 4.3 The Flight Path During the Doppler Radar Trials

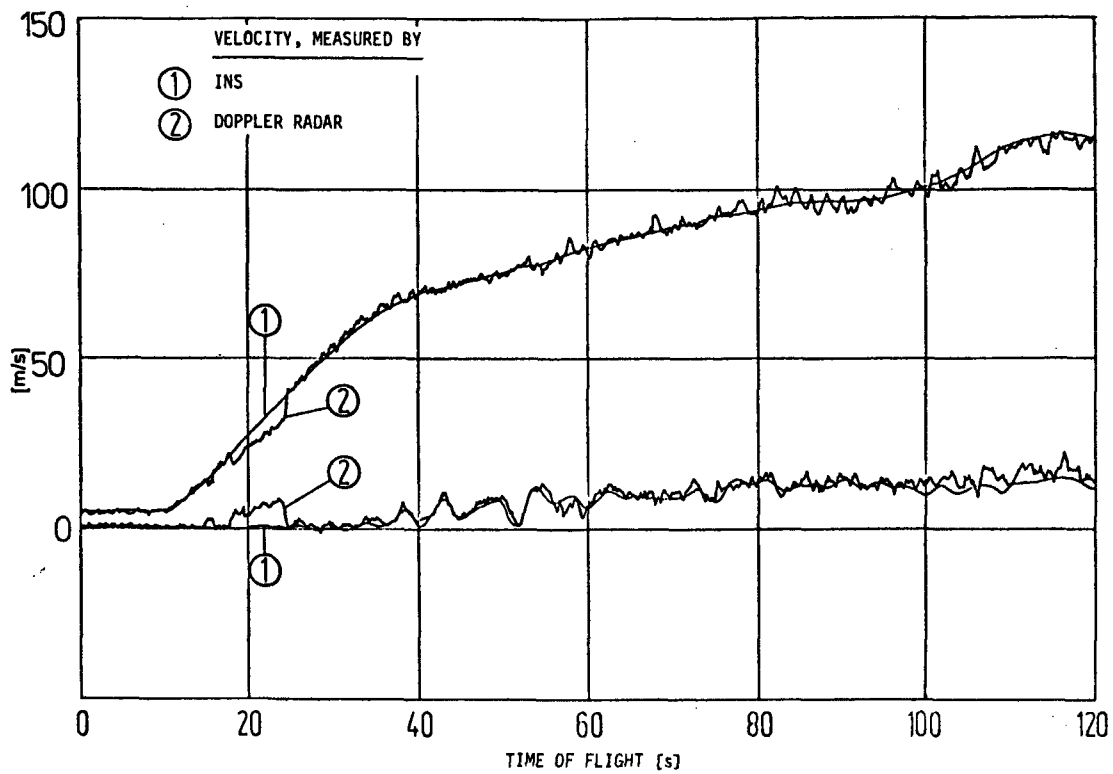


Figure 4.4 The Doppler and the INS Velocity Signals

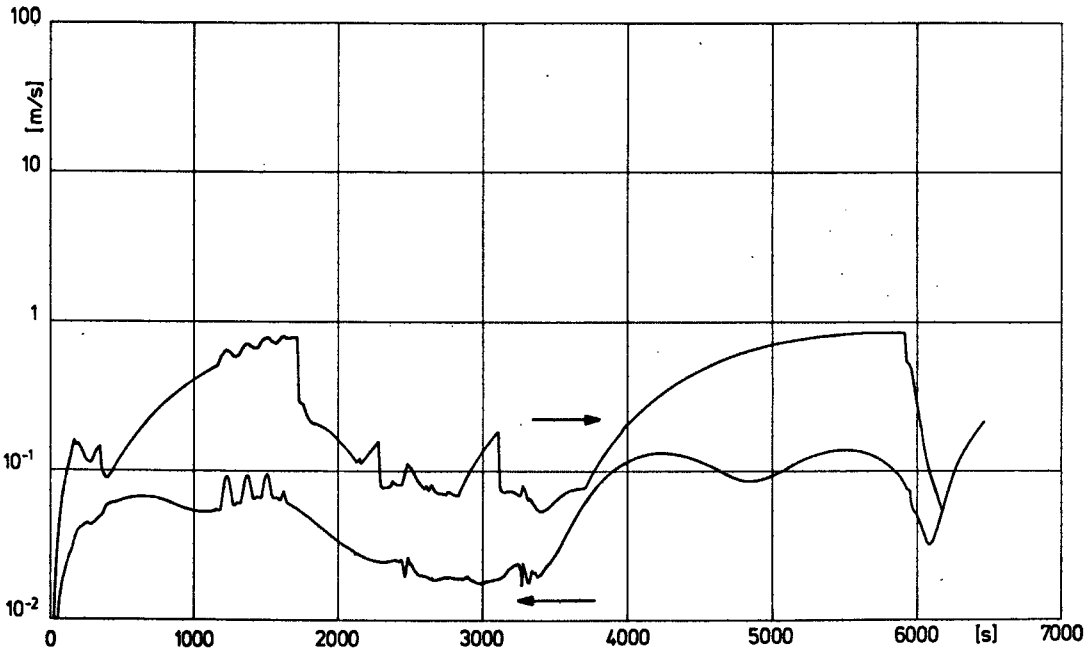


Figure 4.5 1σ - Accuracy Bands for the Reference Velocity Obtained by Forward Filtering and Forward/Backward Smoothing Algorithms

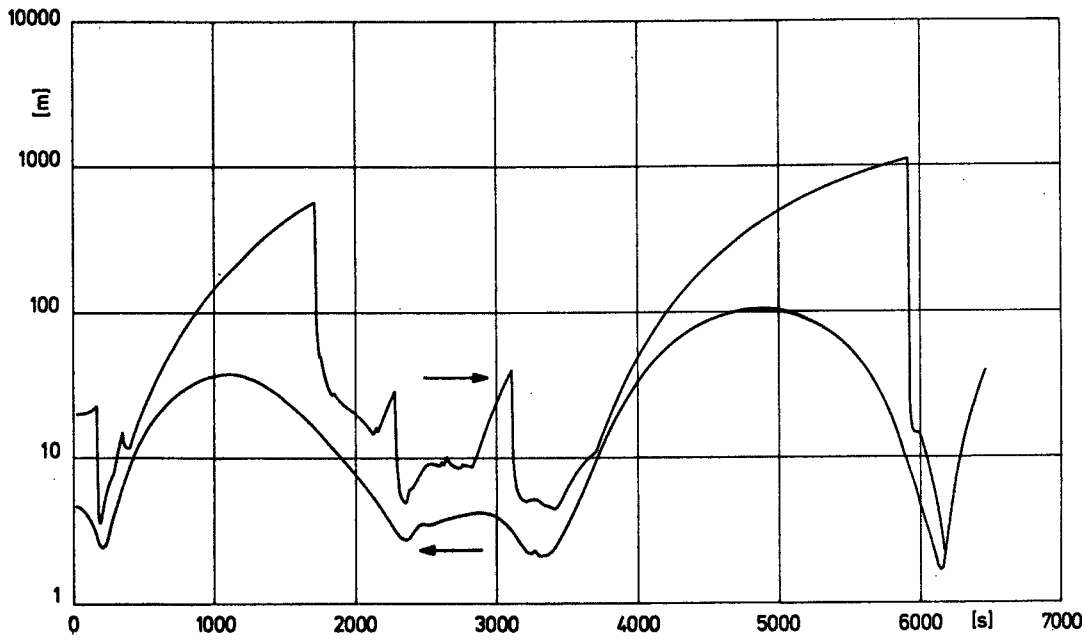


Figure 4.6 1σ - Accuracy Bands for the Reference Flight Path Obtained by Forward Filtering and Forward/Backward Smoothing Algorithms

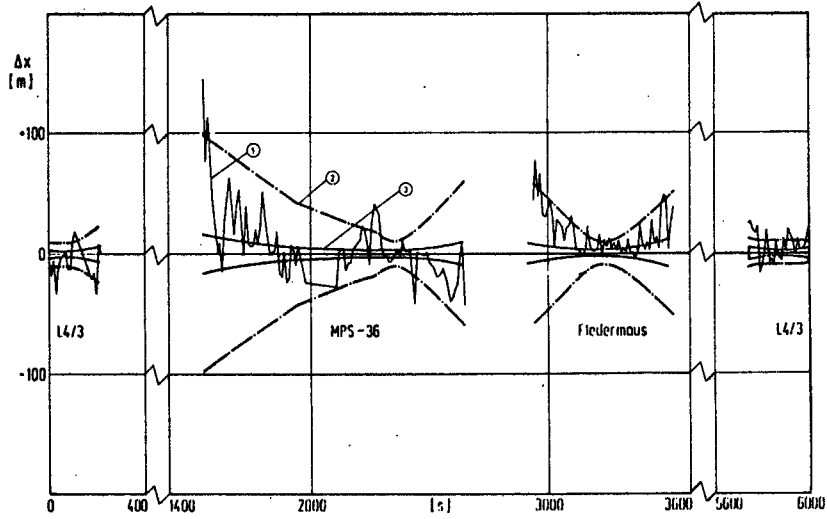


Figure 4.7 Difference between Reference Trajectory and Radar Measurements (1) Plus 1σ - Accuracy Bands for the Radar Measurements (2) and the Reference Flight Path (3)

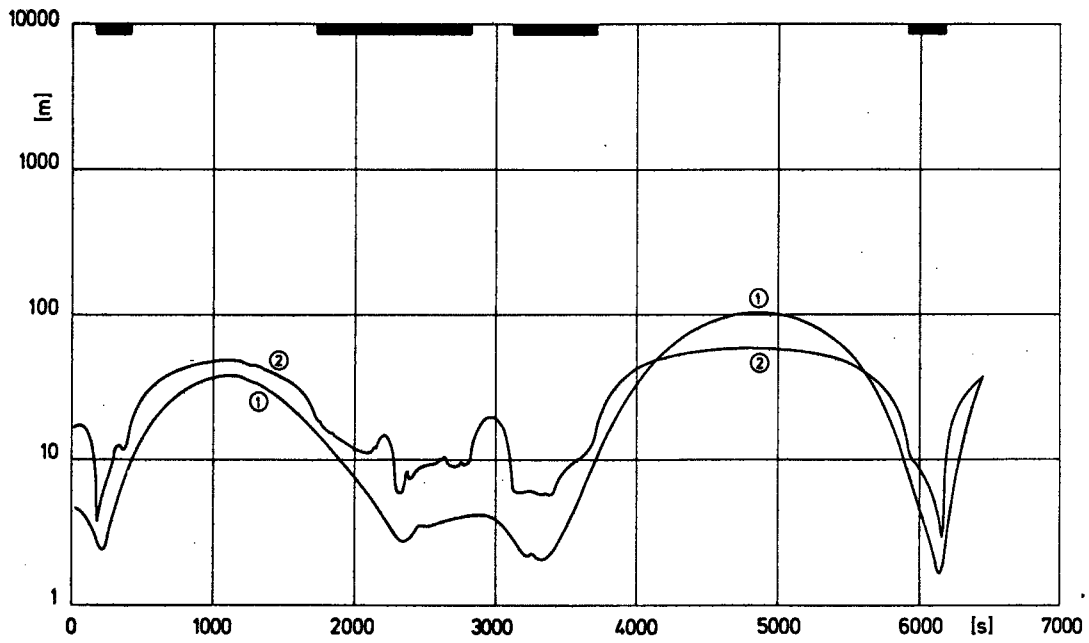


Figure 4.8 1σ - Accuracy Comparison between INS (1) and Doppler Radar Plus Heading Reference (2) Both Aided by Tracking Radar

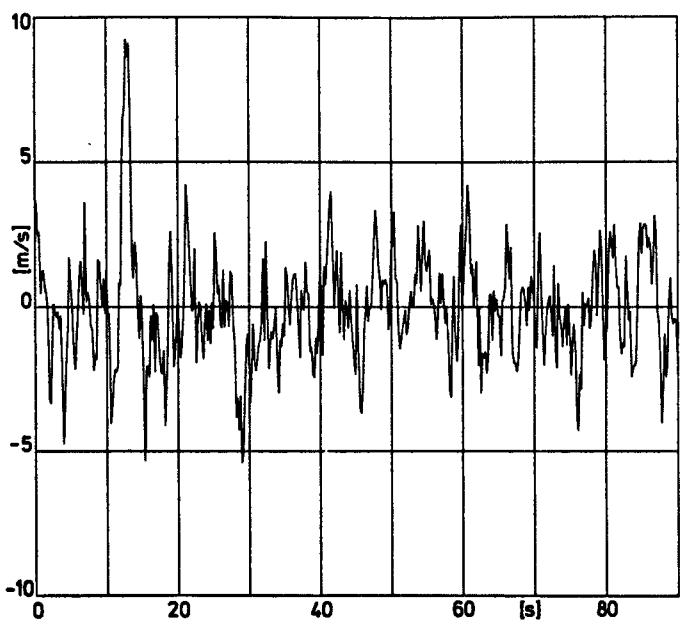


Figure 4.9 Test Results for the Doppler Radar Error over Flat Land

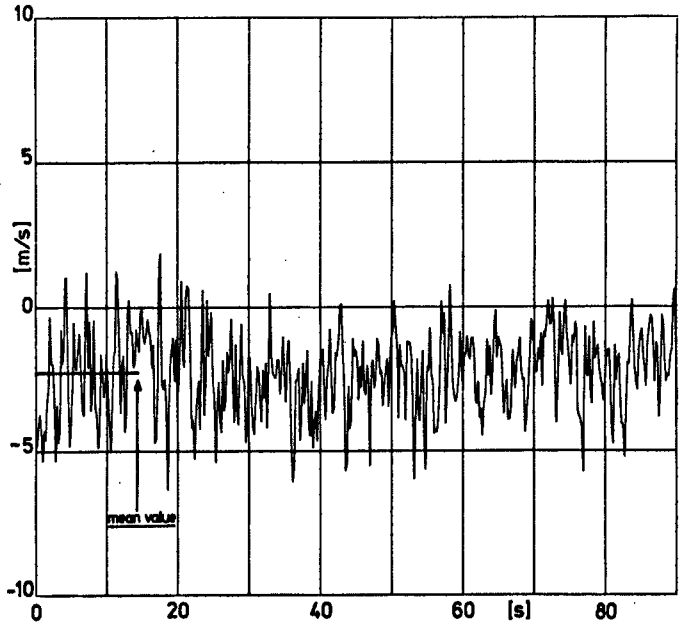


Figure 4.10 Test Results for the Doppler Radar Error over Water

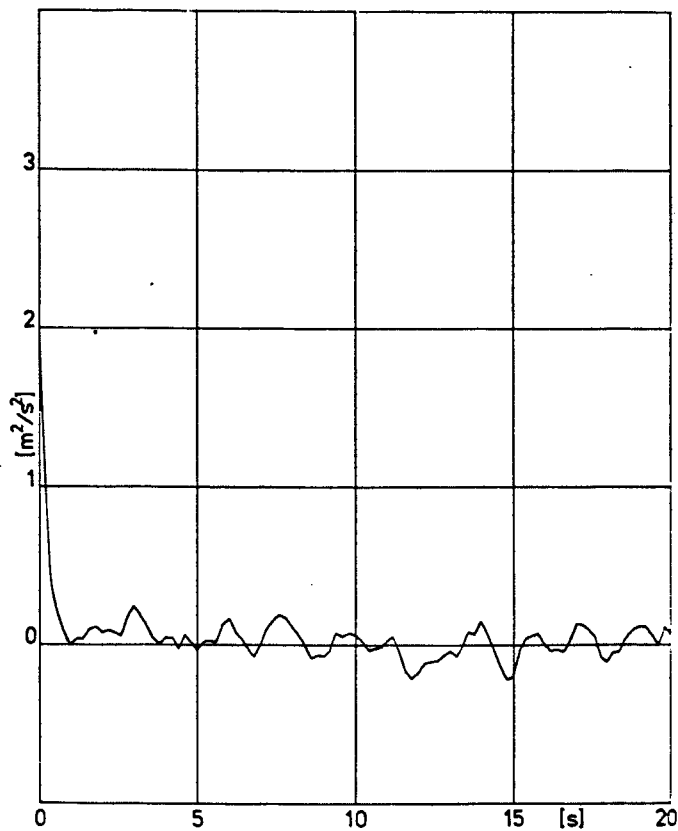


Figure 4.11 Autocorrelation Function of the Doppler Radar Error

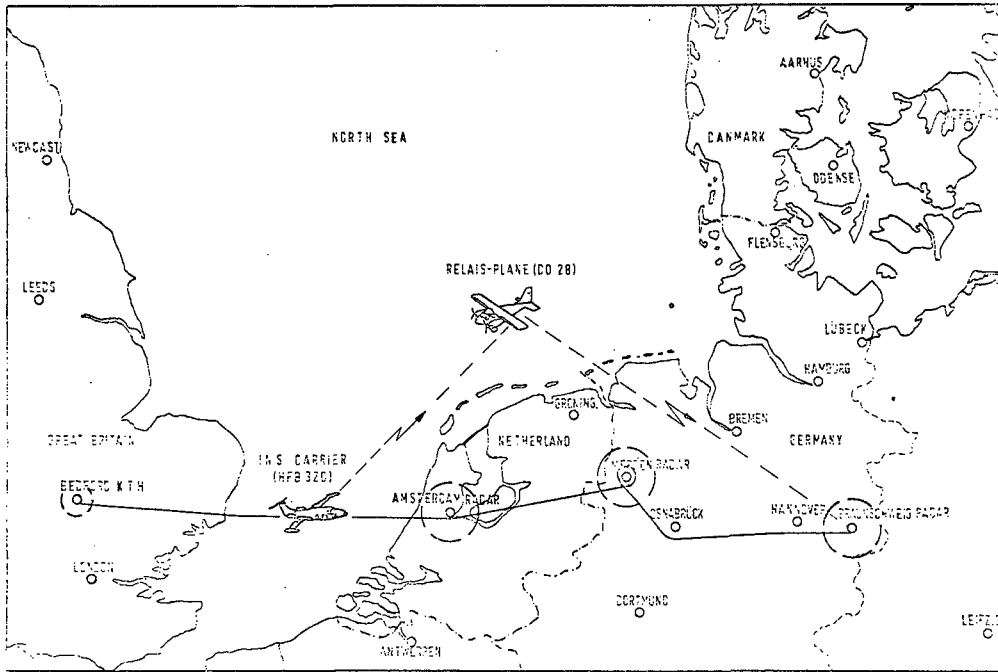


Figure 5.1 The Tracking Facilities and the Telemetry Link During the Long Range INS Flight Tests

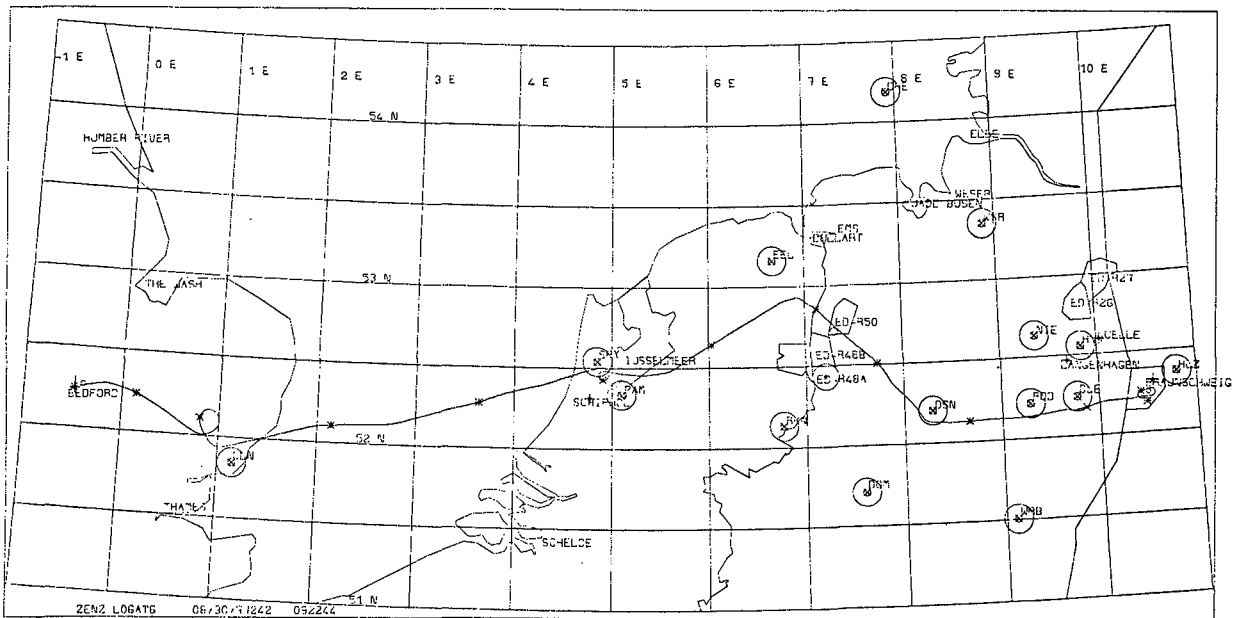


Figure 5.2 The Flightpath from Bedford to Braunschweig

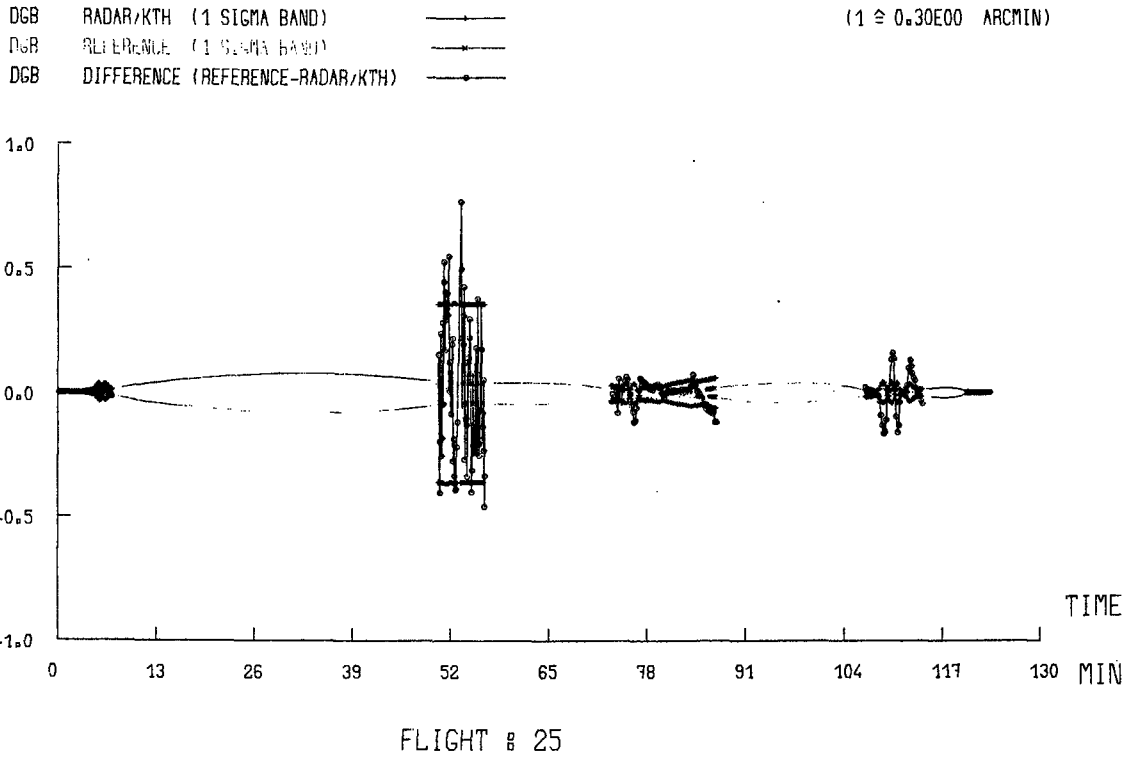


Figure 5.3 The 1σ - Band of the Reference Flightpath and the External Measurements

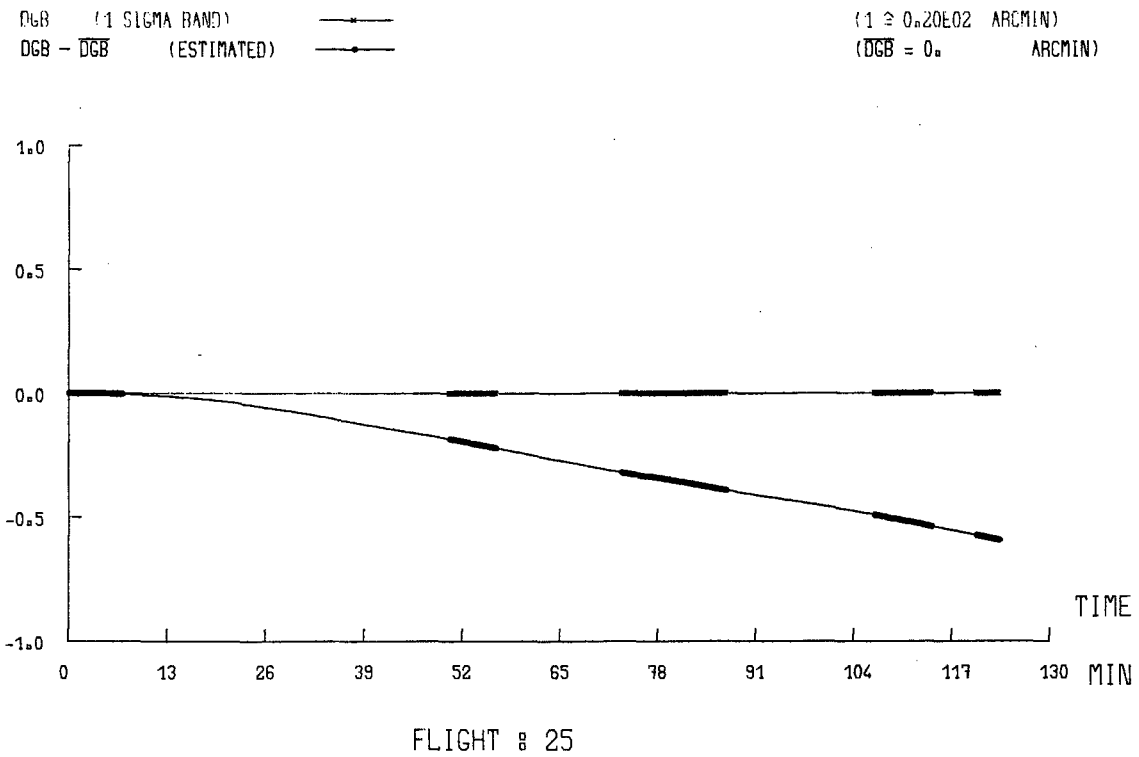


Figure 5.4 1σ - Band and Optimal Estimate for the INS Latitude Error

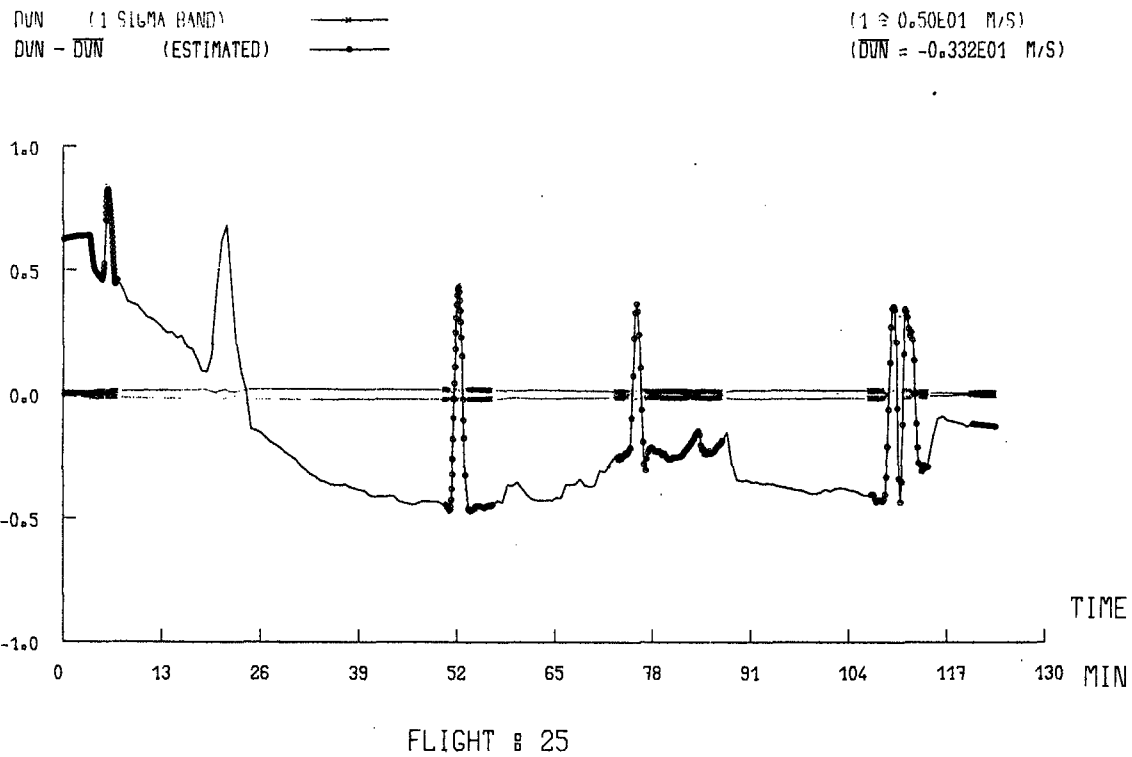


Figure 5.5 1σ - Band and Optimal Estimate for the INS North Velocity Error

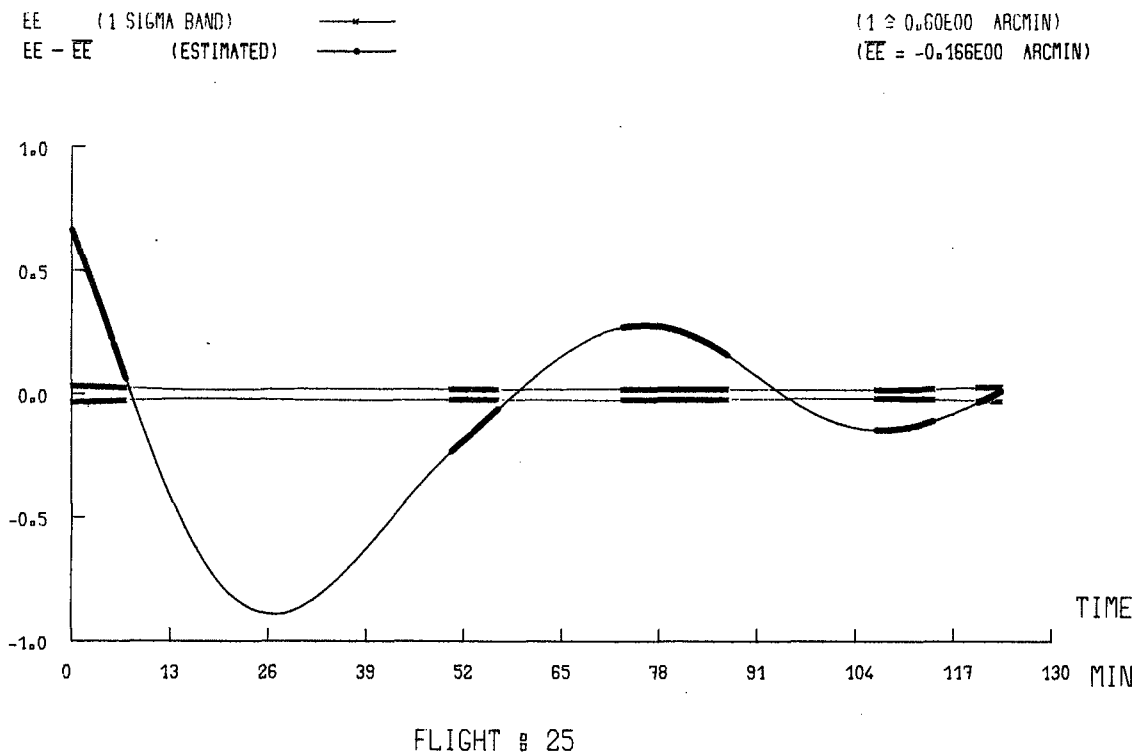

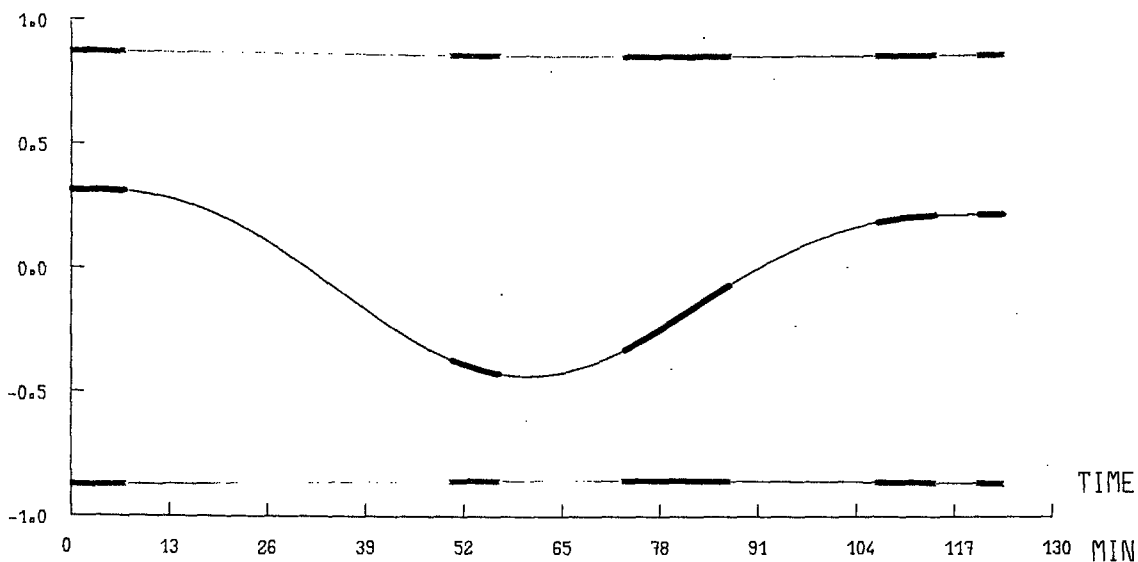


Figure 5.6 1σ - Band and Optimal Estimate for the INS East-West Misalignment

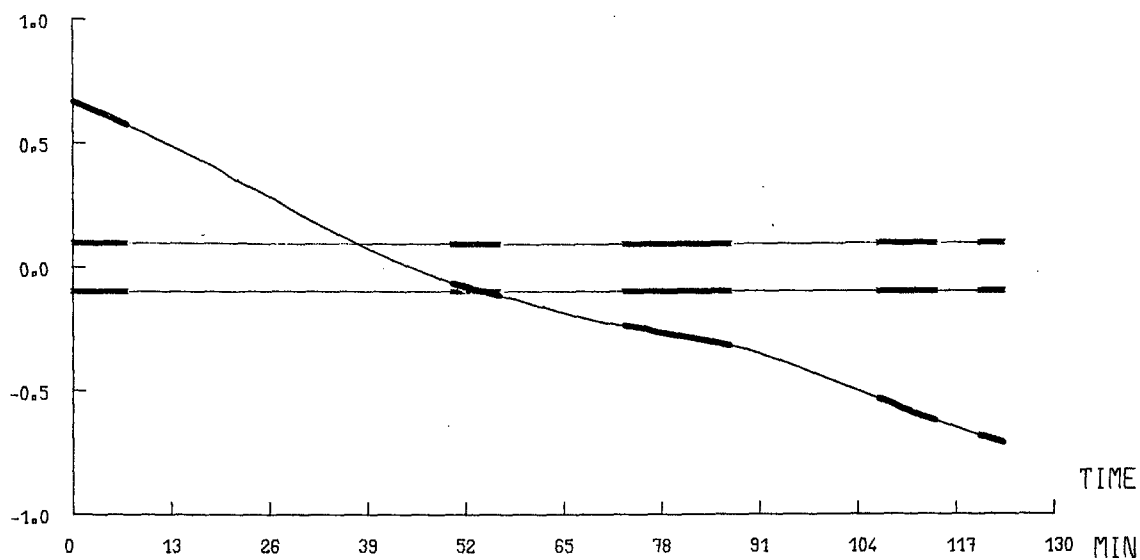
DE (1 SIGMA BAND)  (1 \cong 0.60E-02 DEG/H)
 DE - DE (ESTIMATED)  (DE = 0.328E-01 DEG/H)



FLIGHT # 25

Figure 5.7 1σ - Band and Optimal Estimate for the INS East-West Gyro Drift

EV (1 SIGMA BAND)  (1 \cong 0.20E02 ARCMIN)
 EV - EV (ESTIMATED)  (EV = -0.449E02 ARCMIN)



FLIGHT # 25

Figure 5.8 1σ - Band and Optimal Estimate for the Azimuth Misalignment